



Changes in endogenous phytohormones regulated by microRNA-target mRNAs contribute to the development of Dwarf Autotetraploid Chinese Cabbage (*Brassica rapa* L. ssp. *pekinensis*)

Yiheng Wang¹ · Shengnan Huang¹ · Zhiyong Liu¹ · Xiaoyan Tang¹ · Hui Feng¹

Received: 19 April 2018 / Accepted: 9 August 2018 / Published online: 16 August 2018
© Springer-Verlag GmbH Germany, part of Springer Nature 2018

Abstract

Polyloidization is considered as the major force that drives plant species evolution and biodiversity. The leaves of Chinese cabbage, an important vegetable crop valued for its nutritional quality, constitute the main edible organ. In this study, we found that autotetraploid Chinese cabbage (*Brassica rapa* ssp. *pekinensis*) generated from a doubled haploid (DH) line via isolated microspore culture exhibits a dwarf phenotype, along with thick leaves and delayed flowering. Abscisic acid (ABA) and brassinosteroid (BR) levels were significantly lower in autotetraploids compared to DHs. Comparative transcriptome analysis was performed to examine the gene regulatory network. A total of 13,225 differentially expressed genes (DEGs) were detected. Further microRNA (miRNA) analysis identified 102 DEGs that correspond to 35 differentially expressed miRNAs (DEMs). Subsequent screening of these 102 genes identified 13 key genes with 12 corresponding differentially expressed miRNAs that are related to leaf development and dwarfism. These 13 genes are involved in the regulation of various processes, including BR synthesis (dwarfing), plant growth, flowering time delay, ABA pathway-related growth and metabolism, leaf morphology and development, and cell extension. Two dwarfing-related genes (*BraA01000252* and *BraA05004386*) regulated by two miRNAs (*novel_15* and *novel_54*) were determined to be downregulated, indicating their possible role in leaf thickness and dwarfism in autotetraploid plants. We also propose two possible miRNA-dependent regulatory pathways that contribute to trait formation in autotetraploid Chinese cabbage. These results provide a theoretical basis for further work involving Chinese cabbage varieties by inducing polyploidy.

Keywords Autotetraploid · Chinese cabbage · Transcriptome · MicroRNA · Dwarfism

Introduction

Polyploidy or whole genome duplication (WGD) has played a major role in higher plant evolution and speciation (Doyle et al. 2008; Soltis et al. 2009; Jiao et al. 2011). Genomic studies and comparative genomics indicate that ancient WGDs are ubiquitous and recurrent in the history of angiosperms (Van de Peer et al. 2017). Polyploidy in angiosperms frequently occurs in association with allopolyploidy, which combines the diploid nuclear genomes from two or more different ancestral species or genera to form new species. Autopolyploids originate from doubling of structurally similar and homologous genomes (Jackson 1982; Ramsey and Schemske 2002). Autopolyploids exhibit superior features and allow plants to adapt to environmental changes (Vergara et al. 2017). For example, autotetraploid *Lolium* develops larger leaves by increasing its cell elongation rate, and autotetraploid *Morus* also has greater height, breast-height

Communicated by S. Hohmann.

Yiheng Wang and Shengnan Huang contributed equally to this work and share the first authorship.

Electronic supplementary material The online version of this article (<https://doi.org/10.1007/s00438-018-1480-z>) contains supplementary material, which is available to authorized users.

✉ Hui Feng
fenghuiaaa@263.net

¹ Department of Horticulture, Shenyang Agricultural University, 120 Dongling Road, Shenhe District, Shenyang, SY, China

diameter, and fruits than their diploid progenitors (Sugiyama 2005; Dai et al. 2015). Autotetraploid rice were found causing low pollen fertility and low seed setting (He et al. 2011; Wu et al. 2015, 2017); however, rice breeders have developed neo-tetraploid rice with high fertility and heterosis using autotetraploid rice (Guo et al. 2017).

Polyploidy induction using colchicine is a popular breeding method in various crops (Majdi et al. 2010; Tang et al. 2010). Polyploidy is particularly of significance in plants that are reproduced asexually such as Chinese cabbage, where leaves serve as the primary photosynthetic organs. Chinese cabbage mutants are produced by isolated microspore culture, which not only affects leaf color but also influences photosynthetic efficiency, thereby altering overall plant growth and development (Huang et al. 2014).

Recent reports have indicated that leaf development and dwarfism are regulated by the interaction of various phytohormones. Autotetraploid *Salix viminalis* leaves contain significantly higher contents of gibberellins (GAs) and cytokinins (CTKs) compared to diploids, whereas abscisic acid (ABA) and indoleacetic acid (IAA) contents do not significantly differ (Dudits et al. 2016). Additionally, *trans*-zeatin (TZ), an active cytokinin, with levels varying among individual tetraploid lines, is involved in leaf development (Dudits et al. 2016). Dwarfism has been valuable in enhancing the harvestable yield of various crops (Hedden 2003; Muangprom and Osborn 2004). In oilseed *Brassica napus*, dwarf genes also may be useful in improving yield because many cultivars readily undergo lodging, leading to yield loss and difficulty in harvesting (Muangprom and Osborn 2004). That same study identified a dwarf gene that is involved in the GA pathway and that influenced plant growth. However, hormone levels of IAA and brassinosteroids (BRs) are remarkably lower in dwarf autotetraploid apples, whereas the GA content has no significant difference (Ma et al. 2016). Wang et al. (2017) found that the *DSG1* gene positively regulates cell division and may be involved in multiple hormone pathways in a dwarf rice mutant. Hou and Niu (2017) found that the *CsDET2* gene leads to BR deficiency and induces a compact phenotype in a dwarf cucumber mutant.

Next-generation sequencing technology has been extensively applied to various polyploid plants (Stupar et al. 2007; Zhou et al. 2015; Braynen et al. 2017). Transcriptome analysis of *Arabidopsis thaliana* autotetraploids has shown that gene expression strongly depends on the parental genome and is associated with DNA methylation (Yu et al. 2010). Similarly, some key hormone-related genes that regulate leaf development have been found in woody autotetraploids such as birch (Mu et al. 2012) and mulberry (Dai et al. 2015). Cytological observations and transcriptomic analysis of floral buds in autotetraploid *B. rapa* have identified key genes that are involved in meiosis (Braynen et al. 2017). In

addition, researchers have utilized transcriptome analysis of neo-tetraploid rice to reveal a large number of specific differentially expressed genes (DEGs) associated with heterosis and fertility (Guo et al. 2017). Comparative small RNA analysis of pollen and embryo sac development in autotetraploid rice has identified differentially expressed miRNAs (DEMs) and siRNAs that result in low fertility and poor seed set (Li et al. 2016, 2017). Because miRNAs inhibit their mRNA targets via base pairing, mRNA targets can be predicted using bioinformatics software, and integrated mRNA and miRNA analysis can help in unraveling the molecular network at the transcriptional and post-transcriptional levels (Yang et al. 2016; Chen et al. 2017; Qiao et al. 2017).

To better understand the growth and development of the edible part of Chinese cabbage, namely, the leaves in autotetraploids, we used a Chinese cabbage DH line 'FT', which was generated by isolated microspore culture and created autotetraploid Chinese cabbages that had exactly the same genetic background as DH. Furthermore, we applied RNA-seq for both transcriptomic and miRNA analysis in this study. We also determined the DEGs and DEMs between the doubled haploids (2x) and autotetraploids (4x) libraries and identified critical microRNA-target mRNAs that are involved in hormone regulation, which may result in the dwarf autotetraploid Chinese cabbage.

Materials and methods

Plant materials and ploidy identification

Isolated microspore culture was performed using a Chinese cabbage DH line 'FT', which exhibits heat resistance, white flowers, and leafy heads. The microspore culture protocol was based on our previously described method (Huang et al. 2014).

The regenerated plants (M_0 generation) were transplanted in the field. The M_1 generation seeds were harvested after self-crossing. The ploidy of the M_1 generation plants was identified using a FACSCalibur flow cytometer (Huang et al. 2014), and 2x and 4x plants were obtained, which exhibited stable inheritance after multiple generations.

Histochemical analysis

Samples were the longitudinal sections of the central part of the mature leaves that were collected from the same area of the 2x and 4x plants. Paraffin sections were prepared according to the method of Chen et al. (2015) and were stained using safranin' O/ Fast Green. The slides were observed under an optical microscope (Nikon ECLIPSE 80i, Japan).

Measurement of hormone content

At the bolting stage, mature leaves from the main stem below the first branch were collected from the 2× and 4× plants. The leaves collected from five 2× or 4× plants were pooled into one biological replicate. Three biological replicates of each ploidy were selected for hormone content measurements, including IAA, GA, TZ, ABA, and BR. Endogenous IAA, ABA, TZ, and ABA were quantified as described elsewhere (Chen et al. 2012), whereas endogenous BR was quantified following the method of Ding et al. (2013).

RNA extraction

The samples of measuring hormone contents were the same as those used for transcriptome and miRNA sequencing. Similarly, leaves collected from five 2× or 4× plants were pooled into one biological replicate for sRNA-seq, and three biological replicates were prepared for transcriptome sequencing. Total RNA extraction was performed using TRIzol reagent (Invitrogen, USA) according to the manufacturer's instructions. The integrity of the RNA samples was assessed using the RNA Nano 6000 Assay Kit of the Bioanalyzer 2100 system (Agilent Technologies, CA, USA).

Library construction, transcriptome sequencing, and analysis

For the construction of RNA libraries, 3 µg of RNA per sample was used to generate sequencing libraries using the NEBNext[®] Ultra[™] RNA library prep kit for Illumina[®] (NEB, USA), following manufacturer's recommendations. mRNA was purified from total RNA using poly-T oligo-attached magnetic beads, followed by fragmentation. First- and second-strand cDNAs were synthesized as described by the manufacturer. The remaining overhangs were converted into blunt ends using an exonuclease/polymerase. Hybridization was conducted by ligating the NEBNext adaptor with a hairpin loop structure. cDNA fragments of preferentially 150–200 bp in length were selected by purifying the library fragments with AMPure XP system (Beckman Coulter, Beverly Hills, CA, USA). Then, 3 µL of a USER enzyme (NEB, USA) was employed with size-selected, adaptor-ligated cDNA at 37 °C for 15 min, followed by 5 min at 95 °C before PCR. The PCR products, which were obtained using Phusion High-Fidelity DNA polymerase, universal PCR primers, and an index (X) primer, were purified, and library quality was assessed using the Agilent Bioanalyzer 2100 system.

Raw data were first processed using in-house Perl scripts. Paired-end clean reads were aligned to the reference genome (http://brassicadb.org/brad/datasets/pub/Genomes/Brassica_rapa/V2.0/) using TopHat (v2.0.12). HTSeq v0.6.1 was

used to count the number of reads mapped to each gene. Then, the fragments per kilobase per million mapped reads (FPKM) of each gene was calculated based on the length of the gene and the number of reads that were mapped to this gene. Differential expression analysis of the two groups was performed using the DESeq R package (1.18.0). Genes with an adjusted *P* value of <0.05 were assigned as differentially expressed. Goseq and KOBAS were used to test the statistical enrichment of differentially expressed genes in Gene Ontology (GO) and Kyoto Encyclopedia of Genes and Genomes (KEGG) pathways. The GO terms and KEGG pathways with a corrected *P* value <0.05 were considered significantly enriched.

Library preparation for small RNA (sRNA) sequencing and data analysis

The sRNA libraries were prepared using the NEBNext[®] Multiplex Small RNA Library set for Illumina[®] (NEB, USA), following the manufacturer's recommendations. Approximately 3 µg of total RNA per sample was used as input, and the purified small RNAs were ligated with 5'- and 3'-adaptors at both ends. The ligated sRNAs were further purified and reverse-transcribed into cDNAs. These cDNAs were finally amplified using the LongAmp Taq 2X Master Mix, SR Primer for Illumina, and an index (X) primer. PCR products were purified on an 8% polyacrylamide gel (100 V, 80 min). DNA fragments corresponding to 140–160 bp (the length of small noncoding RNA plus the 3' and 5' adaptors) were recovered and dissolved in 8 µL of elution buffer. Single-end sequencing of sRNA libraries was performed on coded samples using a cBot Cluster Generation System and a TruSeq SR Cluster Kit v3-cBot-HS (Illumina). After cluster generation, the library preparations were sequenced on an Illumina HiSeq 2500 platform, and 50-bp single-end reads were generated.

Raw reads were processed through custom Perl and Python scripts. The small RNA tags were mapped to the reference sequence using Bowtie (Langmead et al. 2009) without mismatches to analyze their expression and distribution on the reference. miRNA expression levels were estimated by transcript per million (TPM). For samples without biological replicates, differential expression miRNA analysis of two samples was determined using the DEGseq (Wang et al. 2010). *P* values were adjusted using *q* values (Storey 2003). *Q* values <0.01 and $|\log_2(\text{fold-change})| > 1$ were set as the threshold for significant differential expression by default. Mapped small RNA tags were used to search for known miRNAs. miRBase 20.0 was used as reference, and modified software mirdeep2 (Friedlander et al. 2011) and srna-tools-cli were used to obtain the potential miRNA and draw secondary structures. The target genes of the miRNAs were predicted using psRobot_tar in psRobot (Wu et al. 2012).

qRT-PCR to validate the transcriptomic and MicroRNAomic data

qRT-PCR was performed to validate the expression level of selected DEGs and DEMs of interest. mRNAs were reverse-transcribed with oligo(dT), and miRNAs were reverse-transcribed with specific stem-loop RT primers (Table S1). The qRT-PCRs were performed on an ABI7300 cycler using FastStart Universal SYBR Green Master (Roche). The reaction conditions were as follows: 95 °C for 10 min, followed by 40 cycles of 95 °C for 15 s and 60 °C for 60 s. Three technical replicates of each reaction were performed, and U6 snRNA was used as endogenous control. The sequences of primers used for qRT-PCR of DEGs and DEMs are listed in Table S1. Primers used for reverse transcription were labeled as -RT. Forward primers for qPCR were labeled as -A, and reverse primers were labeled as -S.

Results

Ploidy analysis and phenotypic characterization

Ploidy analysis of novel leaves and control diploid leaves was performed using flow cytometry analysis. Fig. S1 shows that the DNA content of 2× plants reached a major peak at channel 200. Therefore, the DNA content peak at channel 400 was defined as 4×. At the vegetative growth stage, the 4× plants showed significantly smaller leafy head size with shorter length and lower weight than the 2× plants (Fig. 1a; Table 1). At the reproductive growth stage, the 4× plants showed slower growth and more delayed bolting than the 2× plants (Fig. 1b). We selected mature leaves from the main stem below the first branch at the bolting stage for sequencing because through observation of the entire growth period, there were apparent differences in leaf thickness based on touch and size between the 2× and 4× plants (Fig. 1c; Table 1). Moreover, this stage indicated the transition from vegetative to reproductive growth.

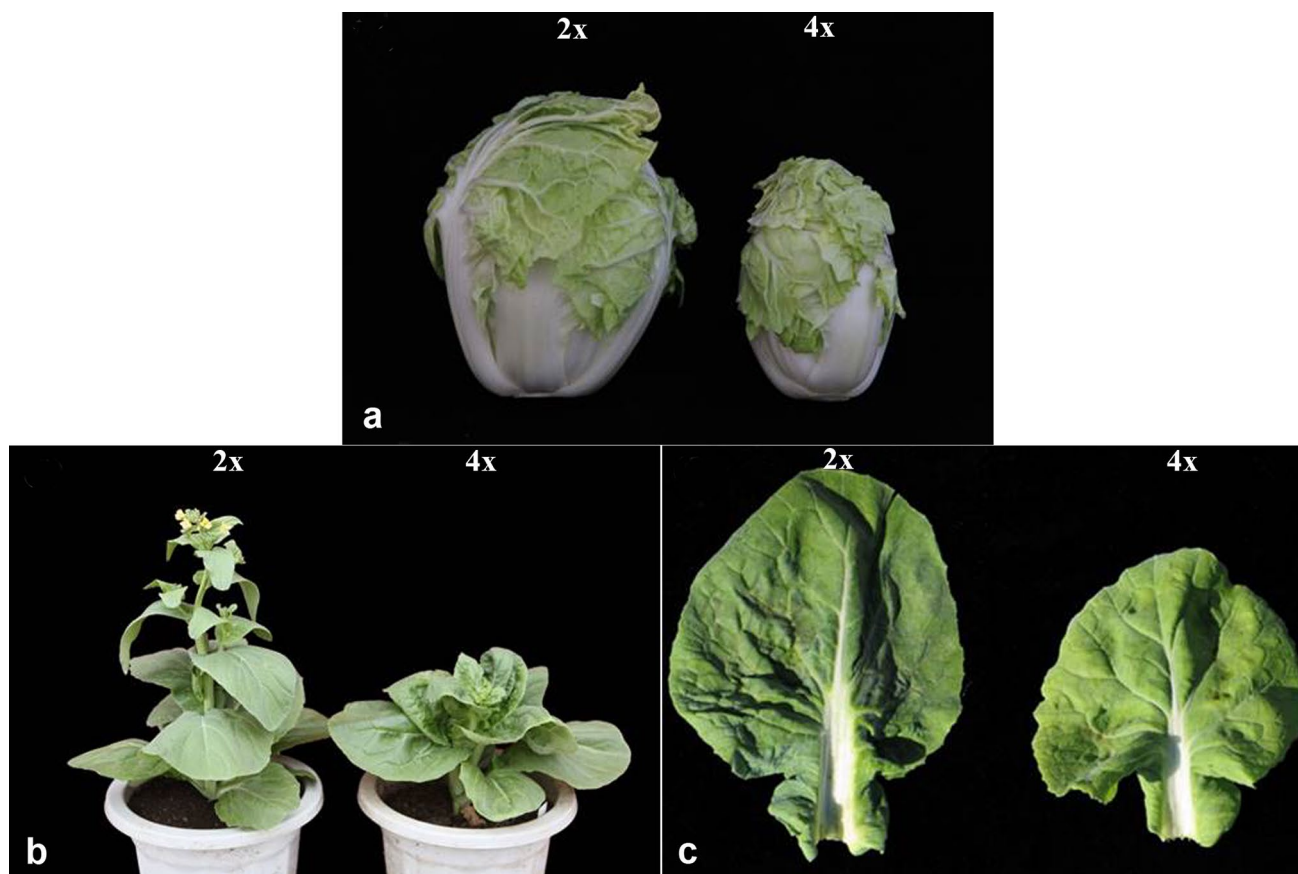


Fig. 1 Plant morphology of 2× and 4× plants. **a** Variation in leafy head size in 2× and 4× plants. **b** Flowering was delayed in 4× plants compared to the 2× plants. **c** Variations in leaf size at the bolting

stage in 2× and 4× plants. Leaves at this stage were sequenced for transcriptomic mRNA and miRNA analyses

Table 1 Phenotypic measurement of 2× and 4× plants (mean ± standard deviation)

	Trait	2× plants	4× plants
Vegetative stage	Plant weight (kg)	0.86 ± 0.05	0.55 ± 0.03**
	Head weight (kg)	0.53 ± 0.02	0.22 ± 0.02**
	Head height (cm)	17.97 ± 0.48	13.66 ± 0.57**
	Head width (cm)	15.87 ± 0.40	9.97 ± 0.28**
Reproductive stage	Leaf length (cm)	21.63 ± 0.82	16.85 ± 0.27**
	Leaf width (cm)	17.45 ± 0.54	13.99 ± 0.37**

** $P < 0.01$ using the student's t test

Histological observation of leaf segments

To explore the cause of autotetraploid thickness, we dissected the leaves of the 2× and 4× plants. The longitudinal sections of the leaf central portion showed that the thickness of the 4× leaves was about 100 μm wider than that of the 2× plants (Fig. 2). Moreover, the cell sizes in the 4× leaves were generally larger than those in the 2× leaves.

Differences in the endogenous hormone levels

We detected common plant hormones that may be associated with leaf development, including IAA, GA, TZ, ABA, and BR. GA was not detected in 2× or 4× plants. We compared the relative levels of endogenous hormones IAA, TZ, ABA,

and BR between the 2× and 4× plants (Table 2). Compared to the 2× plants, IAA and TZ contents in the 4× plants were slightly higher, whereas those of ABA and BR were significantly lower.

Transcriptome analysis

To investigate the genes involved in plant dwarfism and leaf development, transcriptome sequencing was performed. A high degree of reproducibility was observed among the three biological replicates in terms of the number of reads obtained, and approximately 44–54 million reads were obtained in the 2× samples, whereas 48–51 million were generated from the 4× samples (Table S2). After removing the low-quality reads and masking adaptor sequences, about 86.79% of the total reads were mapped to the *Brassica*

Table 2 Levels of endogenous phytohormones (ng/g)

Hormone	2× plants	4× plants
Indole-3-acetic acid	0.587 ± 0.026	0.692 ± 0.114
Trans-zeatin	0.137 ± 0.009	0.147 ± 0.021
Abscisic acid	8.634 ± 0.542	4.997 ± 0.417**
Brassinosteroid	0.034 ± 0.001	0.008 ± 0.001**
Gibberellin	–	–

Data are expressed as the mean ± standard deviation

** $P < 0.01$ using the student's t test

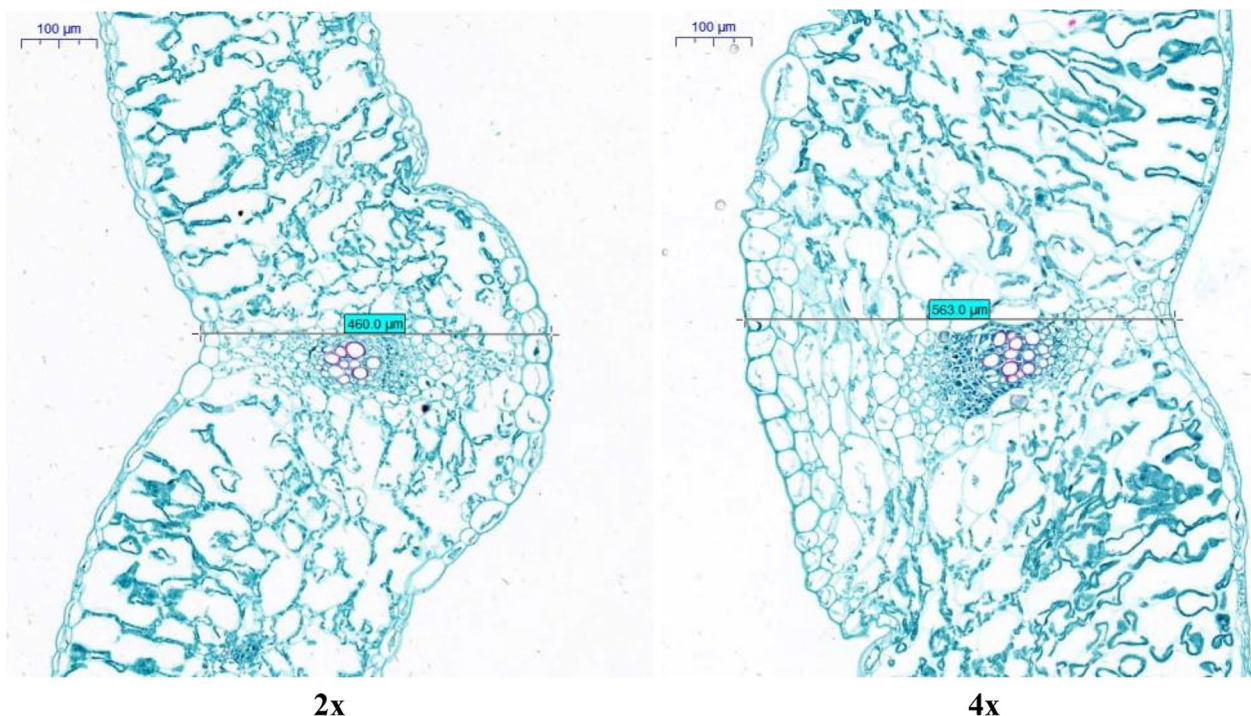


Fig. 2 Longitudinal sections of mature leaf cortices from 2× and 4× plants (×100 magnification)

reference genome. Among these, uniquely mapped reads represented approximately 79.53% of the total reads and were used in the subsequent analysis.

In this study, we identified 13,225 DEGs, of which 6614 were upregulated and 6611 were downregulated (Table S3). To classify the distribution of gene functions in general, a total of 9863 DEGs (74.58%) were assigned to 4157 terms by GO enrichment. Among these, 301 GO terms were significantly enriched based on corrected P value < 0.05 in the DEGs. The 30 most significantly enriched GO terms are shown in Fig. 3. There were 24 terms belonging to the biological processes category. “Biological process” (7291 DEGs) was the predominant group, followed by “metabolic process” (5537 DEGs) and “cellular process” (5368 DEGs). In the molecular function category, “oxidoreductase activity” (1055 DEGs) was the most represented GO term. In the cellular component category, “photosystem II oxygen evolving complex” (33 DEGs) and “oxidoreductase complex” (52 DEGs) were the significantly enriched GO terms.

Pathway-based analysis can further our understanding of the biological functions and gene interactions. All DEGs were mapped to 116 KEGG pathways (Table S4). The most represented was “metabolic pathways” (1,357 DEGs), followed by “biosynthesis of secondary metabolites” (741 DEGs), “ribosome” (262 DEGs), “carbon metabolism”

(237 DEGs), and “biosynthesis of amino acids” (235 DEGs). Among these, “carbon metabolism” was the unique significantly enriched KEGG pathway.

mRNA-miRNA integration analysis

Transcriptome analysis identified a large number of DEGs. To further investigate the regulatory gene network associated with plant dwarfism and leaf development, we measured miRNA levels from sRNA-seq data in the 2× and 4× plants. A total of 4,443,855 and 8,670,601 sRNA reads were obtained, which represented 964,954 and 1,781,718 unique reads in the 2× and 4× libraries, respectively (Table S5). This showed that nearly twice the amount of sRNA was active in the 4× plants compared to the 2× plants. For miRNA analysis, a total of 56 DEMs were detected, including 25 known and 31 novel miRNAs (Table S6).

To explore the biological significance of DEGs and DEMs, comprehensive analysis was performed to elucidate their relationship. An integrated analysis showed only 102 DEGs corresponding to 35 DEMs (Table S7). To elucidate the traits involved in leaf growth and development from our sequencing data and the associated biological processes, functional classification of differentially expressed (DE) miRNAs-target mRNAs was performed using KEGG

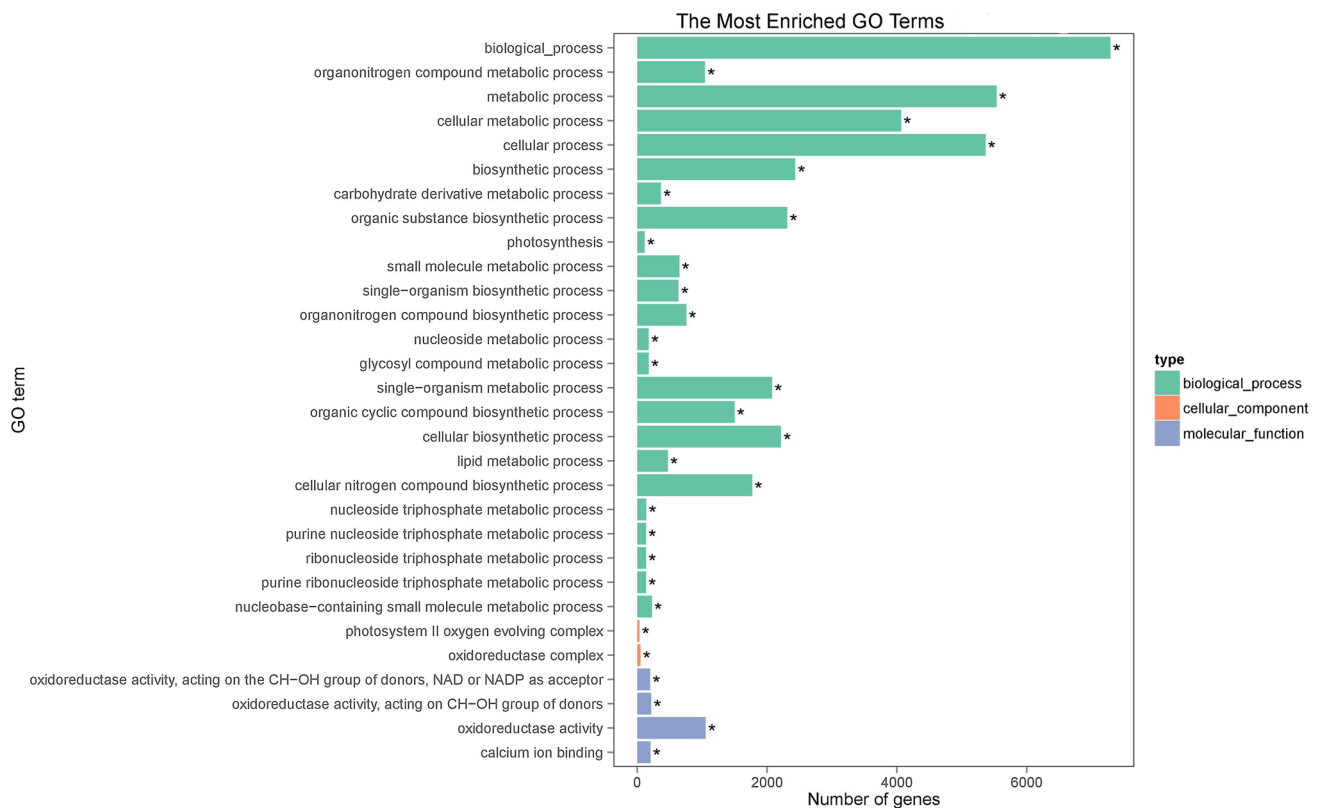


Fig. 3 The 30 most significantly enriched GO terms among 13,225 differentially expressed genes in doubled haploids and autotetraploids

pathway enrichment analysis (Fig. 4). KEGG analysis indicated that a total of 36 pathways were enriched, and the top 20 terms were mainly related to the metabolic pathway, glycolysis/gluconeogenesis, fructose and mannose metabolism, pentose phosphate pathway, BR biosynthesis, and inositol phosphate metabolism. These key pathways contain several critical genes that are possibly involved in leaf development in Chinese cabbage.

Using the Basic Local Alignment Search Tool (BLAST) and gene function annotation, we found that 13 of the 102 DEGs are related to leaf development, including those for BR synthesis, dwarfing, regulation of flowering time, ABA regulation, cell size, leaf development, and leaf tissue formation (Table 3). Furthermore, we identified 13 DEGs that were regulated by 12 DEMs. Among these, two DEMs (*novel_15* and *novel_54*) were upregulated, and

their three target DEGs (*BraA01000252*, *BraA09000469*, and *BraA05004386*) were downregulated, which are involved in BR synthesis and cell elongation, thereby possibly resulting in dwarfism. Another two DEMs (*novel_42* and *novel_44*) targeted two DEGs (*BraA07001177* and *BraA09003100*, respectively), which are probably related to leaf shape and metabolite changes along with dwarfism (Fig. 5). Five DEMs (*bra-miR5720*, *novel_167*, *bra-miR172a*, *bra-miR172c-3p*, and *bra-miR172d-3p*) targeted seven DEGs (*BraA05002597*, *BraA10001056*, *BraA10002300*, *BraA06001479*, *BraA03001002*, *BraA10001990*, and *BraA07001666*) that are involved in the ABA metabolic pathway, leaf formation, and flowering regulation (Fig. 6). Three DEMs (*bra-miR171e*, *novel_35*, and *novel_103*) downregulated one DEG (*BraA03002481*), which may be a transcription factor that is involved in plant development.

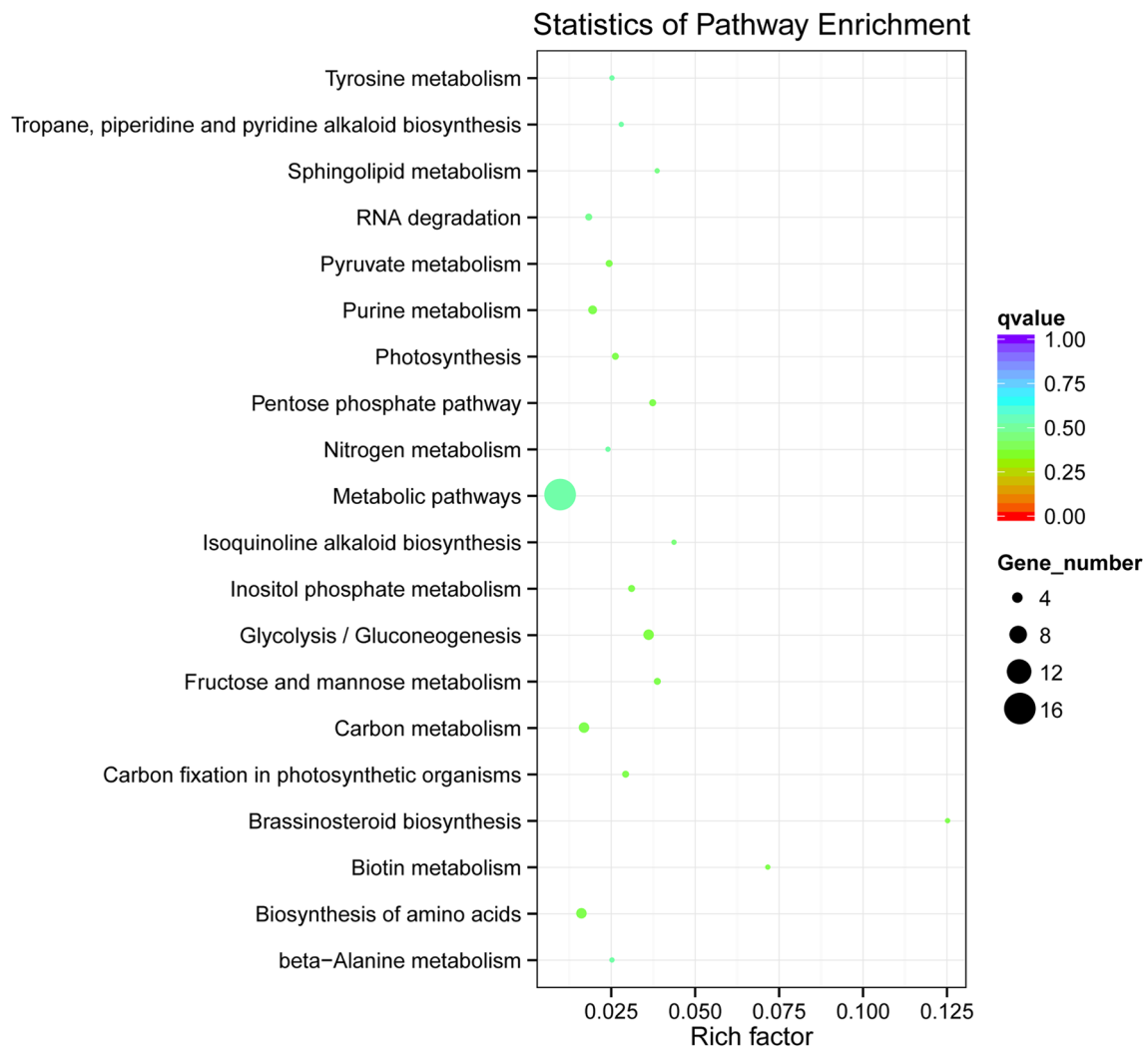
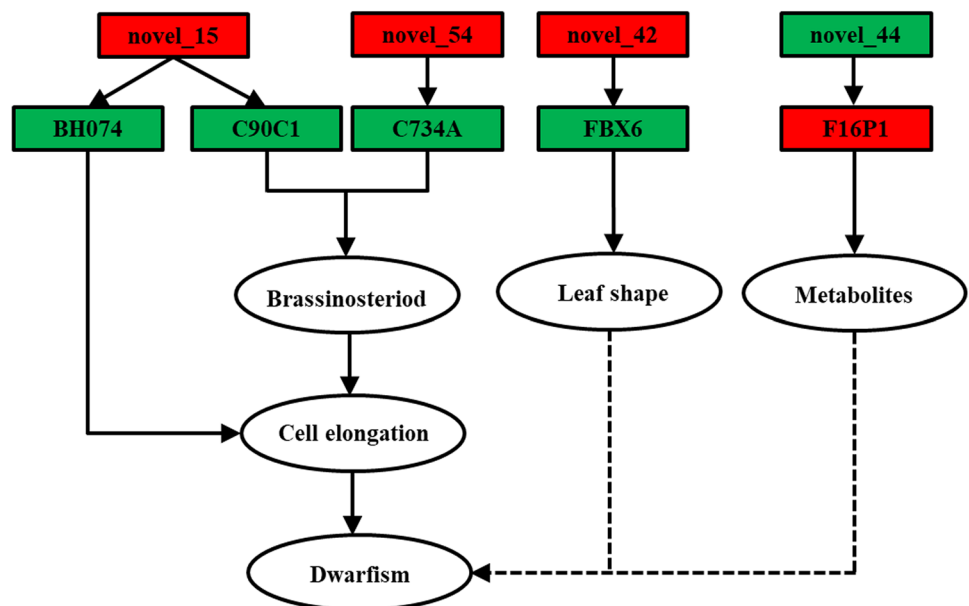


Fig. 4 The top 20 enriched KEGG pathways among 102 differentially expressed genes in doubled haploids and autotetraploids

Table 3 Expression profiles of 13 differentially expressed genes with related 12 differentially expressed miRNAs

Gene ID	Read count (4×)	Read count (2×)	Log2 fold-change (4×/2×)	Related miRNA	Gene description
<i>BraA01000252</i>	2.35	10.94	-2.22	<i>novel_15</i>	C90C1_ARATH 3-epi-6-deoxocathasterone 23-monooxygenase
<i>BraA05004386</i>	306.89	677.75	-1.14	<i>novel_54</i>	C734A_ARATH Cytochrome P450 734A1
<i>BraA03001002</i>	284.79	197.86	0.53	<i>bra-miR172d-3p</i>	MPC1_ARATH Mitochondrial pyruvate carrier 1
<i>BraA06001479</i>	3961.85	2514.10	0.66	<i>novel_167</i>	Y5224_ARATH Uncharacterized protein At5g02240
<i>BraA10002300</i>	636.56	539.28	0.24	<i>bra-miR5720</i>	TAP46_ARATH PP2A regulatory subunit TAP46
<i>BraA10001990</i>	185.40	233.43	-0.33	<i>bra-miR172a</i>	TOE2_ARATH
<i>BraA07001666</i>	45.55	78.50	-0.79	<i>bra-miR172c-3p</i>	AP2-like ethylene-responsive transcription factor
				<i>bra-miR172d-3p</i>	TOE3_ARATH AP2-like ethylene-responsive transcription factor
<i>BraA05002597</i>	1219.19	1482.29	-0.28	<i>bra-miR5720</i>	VCS_ARATH Enhancer of mRNA-decapping protein 4
<i>BraA10001056</i>	740.46	1018.68	-0.46		HUAL1_ARATH HUA2-like protein 1
<i>BraA09003100</i>	11315.11	5408.13	1.07	<i>novel_44</i>	F16P1_ARATH Fructose-1,6-bisphosphatase, chloroplastic
<i>BraA09000469</i>	22.62	51.05	-1.17	<i>novel_15</i>	BH074_ARATH Transcription factor bHLH74
<i>BraA07001177</i>	12.28	26.07	-1.09	<i>novel_42</i>	FBX6_ARATH F-box only protein 6
<i>BraA03002481</i>	261.94	505.28	-0.95	<i>bra-miR171e</i> <i>novel_103</i> <i>novel_35</i>	SCL27_ARATH Scarecrow-like protein 27

Fig. 5 Possible miRNA-dependent regulatory pathways that participate in dwarfism. Solid lines with arrows indicate direct actions, and dotted lines indicate indirect actions. Red represents miRNAs upregulated in 4× vs. 2× plants, and green represents downregulated miRNAs downregulated in 4× vs. 2× plants. (Color figure online)



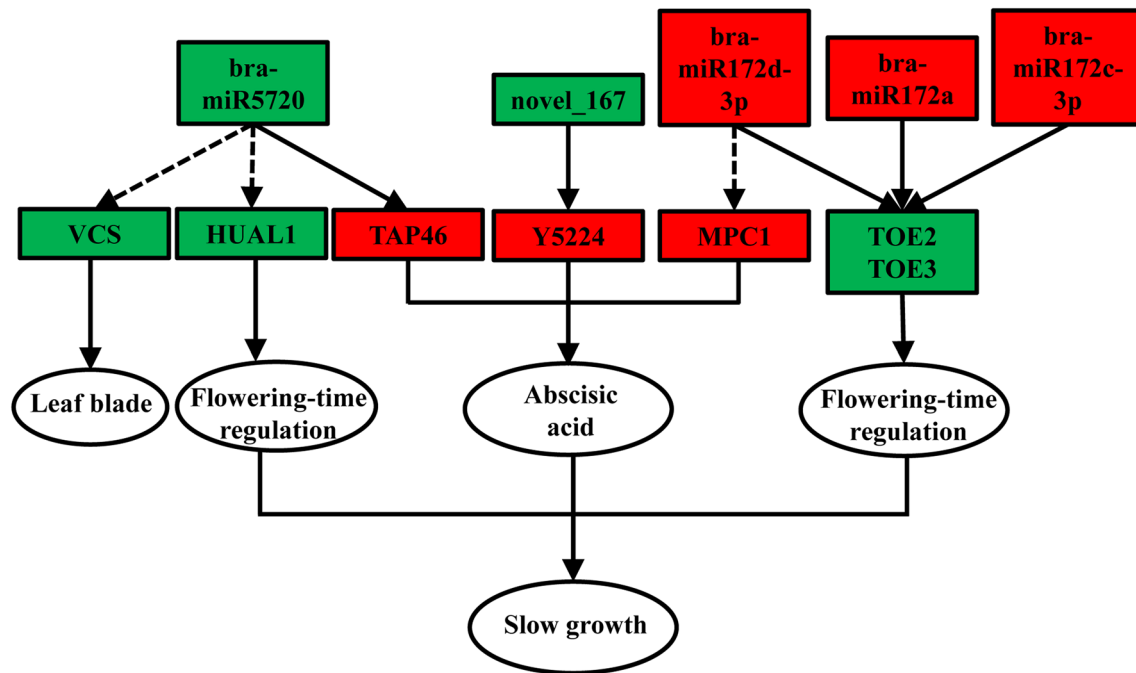


Fig. 6 Possible miRNA-dependent regulatory pathways that participate in leaf development and slow growth. Solid lines with arrows indicate direct actions, and dotted lines indicate indirect actions. Red

represents miRNAs upregulated in 4× vs. 2× plants, and green represents miRNAs downregulated in 4× vs. 2× plants. (Color figure online)

qRT-PCR validation of mRNA and miRNA levels

To confirm the results of transcriptome and miRNA analyses, seven DEGs and seven DEMs that were involved in leaf development and dwarfism were selected. The observed changes in the RNA expression patterns by qRT-PCR coincided with those of RNA-seq analyses, indicating the accuracy of our transcriptomic and microRNAomic data (Figs. S2a, b). However, *BraA10002300* and *BraA03001002* did not show significant differences in gene expression between the 2× and 4× plants.

Discussion

In this study, we created dwarf autotetraploid Chinese cabbages by isolated microspore culture. Because autotetraploids are generated from the spontaneous chromosome doubling of DHs, their genes originated from the same genome, and their genetic backgrounds are theoretically identical. Therefore, this is the most ideal material for investigating ploidy differences. Alterations in gene expression levels absolutely result from ploidy differences, which cause changes in the observed traits between DHs and autotetraploids. Morphological and histochemical analyses showed that the leaves of 4× plants were smaller and thicker than those of 2× plants, and the weight of 4x plants was lower

than that of 2× plants, which differs from the findings of Shahid et al. (2013), who reported that panicle length and leaf area significantly increased, but plant dry weight significantly decreased in autotetraploid rice. The reason for this observed discrepancy requires further investigation. In addition, our physiological and transcriptome-miRNA integrative data indicate that the BR and ABA levels in the 4× plants were significantly lower than those in 2× plants, and 13 DEGs with 12 DEMs regulated the hormone levels that influence leaf development, possibly resulting in dwarf autotetraploid Chinese cabbages.

Dwarfism is an apparent character in our autotetraploid plants. We selected some critical related genes to interpret this phenomenon, combined with data on hormone levels. Two novel miRNAs, *novel_15* and *novel_54*, regulate two critical genes (*BraA01000252* and *BraA05004386*) that are involved in BR synthesis. Functional annotation identified one gene as 3-epi-6-deoxocathasterone 23-monooxygenase (CYP90C1) and the other as cytochrome P450 (CYP734A). *BraA01000252* is the homolog of *ROTUNDIFOLIA3* (*ROT3*) gene in *Arabidopsis*. *ROT3* encodes for the enzyme CYP90C1, which regulates leaf length in *A. thaliana* and is required for later steps in the BR biosynthesis pathway. *ROT3* appears to be required for the conversion of typhasterol to castasterone, an activation step in the BR pathway (Kim et al. 2005). CYP734A1 inactivates brassinolide and castasterone by hydroxylating carbon-26

(C-26) of the substrate side-chain (Turk et al. 2003) and has been identified as a BR-inactivating enzyme that plays an important role in steroid-mediated signal transduction in *A. thaliana* (Thornton et al. 2010). In addition, one DEG (*BraA09000469*) is regulated by *novel_15*, which is annotated as a helix-loop-helix (bHLH) transcription factor that plays an important role in the control of cell elongation in *A. thaliana* (Ikeda et al. 2012). BRs are plant hormones that regulate various physiological processes in plants such as cell expansion and leaf growth and development (Fariduddin et al. 2013). In our study, the downregulation of *BraA01000252* and *BraA05004386* transcripts caused by the upregulation of *novel_15* and *novel_54* may lead to the inhibition of BR synthesis, which possibly affects leaves and cause dwarf autotetraploid plants.

Another two DEGs (*BraA07001177* and *BraA09003100*) are regulated by two DEMs (*novel_42* and *novel_44*, respectively), and were annotated as F-box-only protein 6 and fructose-1,6-bisphosphatase. An F-box gene (*LEAF CURLING RESPONSIVENESS*, *LCR*) regulates leaf morphology, and loss-of-function *lcr* mutants exhibit pleiotropic defects with semi-dwarfism, altered leaf shape, and a shorter stem in *Arabidopsis thaliana* (Song et al. 2012). Fructose-1,6-bisphosphatases (FBPases) are involved in starch and sucrose synthesis and also disrupt both chloroplastic and cytosolic FBPase genes, resulting in starch and metabolite changes along with a dwarf phenotype (Rojas-González et al. 2015). Thus, these two DEGs with their DEMs may indirectly influence dwarf autotetraploid formation. Similarly, the BR content was significantly lower in the 4× plants compared to the 2× plants. These findings suggest that miRNA-dependent regulatory pathways contribute to dwarfism.

Along with the dwarf phenotype, the autotetraploids also showed slow growth. We utilized sequencing data to identify related genes that are responsible for this characteristic. ABA accumulates in senescent tissues during plant growth. In this study, the 4× plants showed slower growth and looked much younger than the 2× plants. Thus, compared to the 2× plants, the 4× plants exhibited significantly lower ABA levels at the same reproductive stage. Similar results were observed in autotetraploid tomatoes (Tal 1977). In our study, three ABA-related target genes were upregulated. We identified *bra-miR5720* as a transcriptional regulator of the *TAP46* gene, which is related to ABA sensitivity in seed germination and protein phosphatase 2A (PP2A) activity. *TAP46* is implicated as a positive factor in ABA-regulated gene expression in *Arabidopsis* (Hu et al. 2014). Plants overexpressing *TAP46* exhibit increased ABA sensitivity in seed germination and reduced PP2A activity (Hu et al. 2014). Overexpression of *TAP46* also leads to stimulation of plant growth and increased nitrogen assimilation (Ahn et al. 2015). Another novel miRNA, *novel_167*, regulates the *BraA10001056* gene, which is annotated as the uncharacterized protein

At5g02240 and is also involved in responses to ABA. We also found a DEG (*BraA03001002*) that was annotated as mitochondrial pyruvate carrier 1 (MPC1). MPC negatively regulates ABA-induced guard cell signaling, and its product is transported to the mitochondria of *A. thaliana* leaves (Li et al. 2014). Therefore, *BraA03001002* might be a predominant DEG that significantly decreases ABA levels in 4× plants. ABA regulates approximately 200 loci and thousands of genes, which in turn influence various processes and are implicated in crosstalk with other developmental signals. Thus, ABA-signaling mechanisms may vary among tissues or developmental stages (Finkelstein 2013) and should be studied in more detail in autotetraploids to determine the specific role of ABA in mechanisms regulating plant growth and development.

A known miRNA, *bra-miR5720*, which is related to the varicose (VCS) and HUA2-like protein 1 (HUAL1) in *Arabidopsis* and their two orthologs (*BraA05002597* and *BraA10001056*) in *Brassica*, was downregulated in autotetraploids in our study. Because of the negative correlation between mRNA and miRNA, *bra-miR5720* may not be the main miRNA that regulates both DEGs. VCS, a WD-domain protein, is required during leaf development and plays an essential role in leaf blade formation. *Arabidopsis* with a mutation in *vcs* shows leaf and shoot apical meristem defects (Deyholos et al. 2003). In *A. thaliana*, the *HUA2* gene is required for proper expression of *FLOWERING LOCUS C* (*FLC*), which is a critical regulator of flowering time (Jali et al. 2014). Lack of different *HUA2-like* genes in mutants results in different flowering times (early-flowering and late-flowering). Thus, downregulation of VCS and HUAL1 is probably responsible for the observed reduction in leaf size and delayed flowering in autotetraploids.

Bra-miR172d-3p not only indirectly regulates MPC1, but also regulates AP2-like ethylene-responsive transcription of *bra-miR172a* and *bra-miR172c-3p* in *A. thaliana*. *TARGET OF EAT* (*TOE*) is one of the AP2-like target genes. Different kinds of *TOE* may also cause different flowering times (Aukerman and Sakai 2003). The regulatory mechanism of flowering time regulation is relatively complicated. Based on the identified DEGs and DEMs that are related to the ABA levels and flowering time regulation, we propose a pathway that depicts this relationship.

Functional and pathway assignments of the DE mRNA- and DE miRNAs-mediated targets using KEGG classification reveal numerous physiological and developmental processes, which may play vital roles in response to polyploidy in *B. rapa*. The 13 critical DEGs that we found are involved in several key pathways such as metabolic pathways, biosynthesis of secondary metabolites, BR biosynthesis, RNA degradation, glycolysis/gluconeogenesis, fructose and mannose metabolism, pentose phosphate pathway, carbon fixation in photosynthetic organisms, and

carbon metabolism, which may offer more information in elucidating the mechanism involving the generation of autotetraploid Chinese cabbage.

Our study provides a theoretical basis for the traits of dwarfism and leaf development in Chinese cabbage and proposes two possible miRNA-target mRNA regulatory pathways that participate in trait formation. DEGs and DEMs were identified in this study; however, their roles in different growth periods require further studies. Moreover, identification of novel miRNAs and their corresponding mRNA in the leaf tissues may help in better understanding the mechanisms employed by autotetraploid plants.

Acknowledgements The National Natural Science Foundation of China (Grant No. 31672144) supported this study.

Author contributions HF and ZYL conceived and designed the study; YHW and XYT performed the experiments; YHW wrote the paper; YHW and SNH reviewed and edited the manuscript; All authors read and approved the manuscript.

Compliance with ethical standards

Conflict of interest The authors declare that they have no conflict of interest.

Ethical approval This article does not contain any studies with human participants or animals performed by any of the authors.

Database linking The transcriptome and microRNAome sequencing data were deposited in the NCBI Gene Expression Omnibus (GEO) Database under accession numbers GSE111607 and GSE111610, respectively.

References

- Ahn C, Ahn HK, Pai HS (2015) Overexpression of the PP2A regulatory subunit Tap46 leads to enhanced plant growth through stimulation of the TOR signalling pathway. *J Exp Bot* 66:827–840
- Aukerman MJ, Sakai H (2003) Regulation of flowering time and floral organ identity by a MicroRNA and its APETALA2-like target genes. *Plant Cell* 15:2730–3741
- Braynen J, Yang Y, Wei F, Cao GQ, Shi GY, Tian BM, Zhang XW, Jia H, Wei XC, Wei ZZ (2017) Transcriptome analysis of floral bud deciphered an irregular course of meiosis in polyploidy Brassica rapa. *Front Plant Sci* 8:768
- Chen ML, Fu XM, Liu JQ, Ye TT, Hou SY, Huang YQ, Yuan BF, Wu Y, Feng YQ (2012) Highly sensitive and quantitative profiling of acidic phytohormones using derivatization approach coupled with nano-LC-ESI-Q-TOF-MS analysis. *J Chromatogr B Analyt Technol Biomed Life Sci* 905:67–74
- Chen B, Wang C, Tian Y, Chu Q, Hu C (2015) Anatomical characteristics of young stems and mature leaves of dwarf pear. *Sci Hortic* 186:172–179
- Chen Y, Dong J, Bennetzen JL, Zhong M, Yang J, Zhang J, Li SL, Hao XJ, Zhang ZG (2017) Integrating transcriptome and microRNA analysis identifies genes and microRNAs for AHO-induced systemic acquired resistance in *N. tabacum*. *Sci Rep* 7:12504
- Dai F, Wang Z, Luo G, Tang C (2015) Phenotypic and Transcriptomic Analyses of Autotetraploid and Diploid Mulberry (*Morus alba* L.). *Int J Mol Sci* 16:22938–22956
- Deyholos MK, Cavaness GF, Hall B, King E, Punwani J, Norman J, Sieburth LE (2003) VARICOSE, a WD-domain protein, is required for leaf blade development. *Development* 130:6577–6588
- Ding J, Mao LJ, Wang ST, Yuan BF, Feng YQ (2013) Determination of endogenous brassinosteroids in plant tissues using solid-phase extraction with double layered cartridge followed by high-performance liquid chromatography-tandem mass spectrometry. *Phytochem Anal* 24:386–394
- Doyle JJ, Fligel LE, Paterson AH, Rapp RA, Soltis DE, Soltis PS, Wendel JF (2008) Evolutionary genetics of genome merger and doubling in plants. *Annu Rev Genet* 42:443–461
- Dudits D, Török K, Cseri A, Paul K, Nagy AV, Nagy B, Sass L, Ferenc G, Vankova R, Dobrev P, Vass I, Ayaydin F (2016) Response of organ structure and physiology to autotetraploidization in early development of energy willow *Salix viminalis*. *Plant Physiol* 170:1504–1523
- Fariuddin Q, Yusuf M, Ahmad I, Ahmad A (2013) Brassinosteroids and their role in response of plants to abiotic stresses. *Biol Plant* 58:9–17
- Finkelstein R (2013) Abscisic acid synthesis and response. *Arabidopsis Book*
- Friedlander MR, Mackowiak SD, Li N, Chen W, Rajewsky N (2011) miRDeep2 accurately identifies known and hundreds of novel microRNA genes in seven animal clades. *Nucleic Acids Res* 40:37–52
- Guo HB, Mendrikahy JN, Xie L, Deng JF, Lu ZJ, Wu JW, Li X, Shahid MQ, Liu XD (2017) Transcriptome analysis of Neo-tetraploid rice reveals specific differential gene expressions associated with fertility and heterosis. *Sci Rep* 7:40139
- He JH, Shahid MQ, Chen ZX, Chen XA, Liu XD, Lu YG (2011) Abnormal PMC microtubule distribution pattern and chromosome behavior resulted in low pollen fertility of an intersubspecific autotetraploid rice hybrid. *Plant Syst Evol* 291:257–265
- Hedden P (2003) The genes of the green revolution. *Trends Genet* 19:5–9
- Hou S, Niu HH (2017) A mutant in the CsDET2 gene leads to a systemic brassinosteroid deficiency and super compact phenotype in cucumber (*Cucumis sativus* L.). *Theor Appl Genet* 76:102–103
- Hu R, Zhu Y, Shen G, Zhang H (2014) TAP46 plays a positive role in the ABSCISIC ACID INSENSITIVE5-regulated gene expression in *Arabidopsis*. *Plant Physiol* 164:721–734
- Huang S, Liu Z, Li D, Yao R, Meng Q, Feng H (2014) Screening of Chinese cabbage mutants produced by ⁶⁰Co γ -ray mutagenesis of isolated microspore cultures. *Plant Breeding* 133:480–488
- Ikeda M, Fujiwara S, Mitsuda N, Ohme-Takagi M (2012) A triantagonistic basic helix-loop-helix system regulates cell elongation in *Arabidopsis*. *Plant Cell* 24:4483–4497
- Jackson R (1982) Polyploidy and diploidy: new perspectives on chromosome pairing and its evolutionary implications. *Am J Bot* 69:1512–1523
- Jali SS, Rosloski SM, Janakirama P, Steffen JG, Zhurov V, Berleth T, Clark RM, Grbic V (2014) A plant-specific HUA2-LIKE (*HULK*) gene family in *Arabidopsis thaliana* is essential for development. *Plant J* 80:242–254
- Jiao Y, Wickett NJ, Ayyampalayam S, Chandrabali AS, Landherr L, Ralph PE, Tomsho LP, Hu Y, Liang HY, Soltis PS, Soltis DE, Clifton SW, Schlarbaum SE, Schuster SC, Ma H, Leebens-Mack J, dePamphilis CW (2011) Ancestral polyploidy in seed plants and angiosperms. *Nature* 473:97–100
- Kim YS, Kim TW, Kim SK (2005) Brassinosteroids are inherently biosynthesized in the primary roots of maize, *Zea mays* L. *Phytochemistry* 66:1000–1006

- Langmead B, Trapnell C, Pop M, Salzberg SL (2009) Ultrafast and memory-efficient alignment of short DNA sequences to the human genome. *Genome Biol* 10:R25
- Li CL, Wang M, Ma XY, Zhang W (2014) NRGA1, a putative mitochondrial pyruvate carrier, mediates ABA regulation of guard cell ion channels and drought stress responses in *Arabidopsis*. *Mol Plant* 7:1508–1521
- Li X, Shahid MQ, Wu JW, Wang L, Liu XD, Lu YG (2016) Comparative small RNA analysis of pollen development in autotetraploid and diploid rice. *Int J Mol Sci* 17:499
- Li X, Shahid MQ, Xia J, Lu ZJ, Fang N, Wang L, Wu JW, Chen ZX, Liu XD (2017) Analysis of small RNAs revealed differential expressions during pollen and embryo sac development in autotetraploid rice. *BMC Genom* 18:129
- Ma Y, Xue H, Zhang L, Zhang F, Ou C, Wang F, Zhang ZH (2016) Involvement of Auxin and Brassinosteroid in Dwarfism of Autotetraploid Apple (*Malus × domestica*). *Sci Rep* 6:26719
- Majidi M, Karimzadeh G, Malboobi MA, Omidbaigi R, Mirzaghaderi G (2010) Induction of tetraploidy to feverfew (*Tanacetum parthenium* Schulz-Bip.): morphological, physiological, cytological, and phytochemical changes. *Hortscience* 45:16–21
- Mu HZ, Liu ZJ, Lin L, Li HY, Jiang J, Liu GF (2012) Transcriptomic analysis of phenotypic changes in Birch (*Betula platyphylla*) Autotetraploids. *Int J Mol Sci* 13:13012–13029
- Muangprom A, Osborn TC (2004) Characterization of a dwarf gene in Brassica rapa, including the identification of a candidate gene. *Theor Appl Genet* 108:1378–1384
- Qiao Y, Zhang J, Zhang J, Wang Z, Ran A, Guo H, Wang D, Zhang JL (2017) Integrated RNA-seq and sRNA-seq analysis reveals miRNA effects on secondary metabolism in *Solanum tuberosum* L. *Mol Genet Genomics* 292:37–52
- Ramsey J, Schemske DW (2002) Neopolyploidy in flowering plants. *Annu Rev Ecol Syst* 33:589–639
- Rojas-González JA, Soto-Suárez M, García-Díaz Á, Romero-Puertas MC, Sandalio LM, Mérida Á et al (2015) Disruption of both chloroplastic and cytosolic FBpase genes results in a dwarf phenotype and important starch and metabolite changes in *Arabidopsis thaliana*. *J Exp Bot* 66:2673–2689
- Shahid MQ, Li YJ, Saleem MF, Naeem M, Wei CM, Liu XD (2013) Yield and yield components in autotetraploid and diploid rice genotypes (*indica* and *japonica*) sown in early and late seasons. *Aust J Crop Sci* 7:632–641
- Soltis DE, Albert VA, Leebens-Mack J, Bell CD, Paterson AH, Zheng C, Sankoff D, dePamphilis CW, Wall PK, Soltis PS (2009) Polyploidy and angiosperm diversification. *Am J Bot* 96:336–348
- Song JB, Huang SQ, Dalmay T, Yang ZM (2012) Regulation of leaf morphology by MicroRNA394 and its target LEAF CURLING RESPONSIVENESS. *Plant Cell Physiol* 53:1283–1294
- Storey JD (2003) The positive false discovery rate: A Bayesian interpretation and the q-value. *Ann Stat* 31:2013–2035
- Stupar RM, Bhaskar PB, Yandel B, Rensink W, Hart A, Ouyang S, Veilleuc RE, Busse JS, Erhardt RJ, Buell CR, Jiang JM (2007) Phenotypic and transcriptomic changes associated with potato autopolyploidization. *Genetics* 176:2055–2067
- Sugiyama S (2005) Polyploidy and cellular mechanisms changing leaf size: comparison of diploid and autotetraploid populations in two species of *Lolium*. *Ann Bot* 96:931–938
- Tal M (1977) Physiology of polyploid plants: DNA, RNA, protein, and abscisic acid in autotetraploid and diploid tomato under low and high salinity. *Int J Plant Sci* 2:119–122
- Tang ZQ, Chen DL, Song ZJ, He YC, Cai DT (2010) In vitro induction and identification of tetraploid plants of *Paulownia tomentosa*. *Plant Cell Tissue Organ Cult* 102:213–220
- Thornton LE, Rupasinghe SG, Peng H, Schuler MA, Neff MM (2010) *Arabidopsis* CYP72C1 is an atypical cytochrome P450 that inactivates brassinosteroids. *Plant Mol Biol* 74:167–181
- Turk EM, Fujioka S, Seto H, Shimada Y, Takatsuto S, Yoshida S, Denzel MA, Torres QI, Neff MM (2003) CYP72B1 inactivates brassinosteroid hormones: an intersection between photomorphogenesis and plant steroid signal transduction. *Plant Physiol* 133:1643–1653
- Van de Peer Y, Mizrahi E, Marchal K (2017) The evolutionary significance of polyploidy. *Nat Rev Genet* 18:411–424
- Vergara F, Rymen B, Kuwahara A, Sawada Y, Sato M, Hirai MY (2017) Autopolyploidization, geographic origin, and metabolome evolution in *Arabidopsis thaliana*. *Am J Bot* 104:905–914
- Wang L, Feng Z, Wang X, Wang X, Zhang X (2010) DEGseq: an R package for identifying differentially expressed genes from RNA-seq data. *Bioinformatics* 26:136–138
- Wang N, Xing Y, Lou Q, Feng P, Liu S, Zhu M, Yin W, Fang S, Lin Y, Zhang T, Sang X, He G (2017) Dwarf and short grain 1 encoding a putative U-box protein regulates cell division and elongation in rice. *J Plant Physiol* 209:84–94
- Wu HJ, Ma YK, Chen T, Wang M, Wang XJ (2012) PsRobot: a web-based plant small RNA meta-analysis toolbox. *Nucleic Acids Res* 40:W22–W28
- Wu JW, Shahid MQ, Chen L, Chen ZX, Wang L, Liu XD, Lu YG (2015) Polyploidy enhances F1 pollen sterility loci interactions that increase meiosis abnormalities and pollen sterility in autotetraploid rice. *Plant Physiol* 169:2700–2717
- Wu JW, Chen L, Shahid MQ, Chen MY, Dong QL, Li JR, Xu XS, Liu XD (2017) Pervasive interactions of *Sa* and *Sb* loci cause high pollen sterility and abrupt changes in gene expression during meiosis that could be overcome by double neutral genes in autotetraploid rice. *Rice* 10:49
- Yang J, Zhang F, Li J, Chen JP, Zhang HM (2016) Integrative Analysis of the microRNAome and transcriptome illuminates the response of susceptible rice plants to rice stripe virus. *PLoS One* 11:e0146946
- Yu Z, Haberer G, Matthes M, Rattei T, Mayer FX, Gierl A et al (2010) Impact of natural genetic variation on the transcriptome of autotetraploid *Arabidopsis thaliana*. *Proc Natl Acad Sci* 107:17809–17814
- Zhou Y, Kang L, Liao S, Pan Q, Ge X, Li Z (2015) Transcriptomic analysis reveals differential gene expressions for cell growth and functional secondary metabolites in induced autotetraploid of Chinese woad (*Isatis indigotica* Fort.). *PLoS One* 10:e0116392